horizontals at 330–360 °C and 470 °C onward. The corresponding loss of weights have been found to be 40.1% and 62.1%, respectively, due to the expulsion of one urea at each step (calculated 39.9% and 60.8%, respectively). The ultimate product has been found to be MnF_3. No further loss of weight between 470 and 800 °C suggests that MnF_3 once formed in this process does not undergo any change in the range of temperature involved in the present TGA experiment. The information hitherto obtained may be useful for the solid-state synthesis of the intermediates $[MnF_3(urea)_2]$ and $[MnF_3(urea)]$. Further, pyrolysis of $[MnF_3(urea)_2]\cdot 3H_2O$ at ca. 500 °C, under nitrogen, leading to MnF_3 appears to be an useful way of accessing this compound. It may be relevant to add that this route to MnF_3 is simpler than the literature method,[48] and the compound is important as a powerful fluorinating agent.[49]

Concluding Remarks

Fluoride-assisted stabilization of manganese(III) has been demonstrated by synthesizing a large number of mixed-ligand fluoro compounds of the metal from aqueous solutions. The coligands have been drawn from $C_2O_4^{2-}$, EDTA, HPO_4^{2-}, glycine, 2,2′-bipyridine, 1,10-phenanthroline, and urea, and the importance of the chemical determination of the oxidation state of the metal in such compounds has been emphasized. Each of the newly synthesized complexes has a distorted octahedral structure. An internal comparison of magnetic moments of $[MnF_5]^{2-}$,[4] $[MnF_3(SO_4)]^{2-}$,[13] $[MnF_3(C_2O_4)]^{2-}$,[17] and $[MnF_3(urea)_2]\cdot 3H_2O$ and the other compounds reported herein led to a qualitative magnetostructural correlation. Thus, for a fluoro- or mixed-ligand fluoromanganese(III) species, the magnetic moment appears to be normal when there is no intermolecular fluoro bridge; however, if there is any -Mn-F-Mn-F- interaction in the crystal lattice there exists a finite possibility of antiferromagnetism. Pyrolysis of $[MnF_3(urea)_2]\cdot 3H_2O$ at ca. 500 °C affords MnF_3, a compound of acknowledged importance as a potential fluorinating agent. This route to MnF_3 is simpler than the literature method.[48] The molecular mixed-ligand fluoromanganese(III) complexes are expected to show interesting oxidation reactions.

Acknowledgment. We thank the CSIR, New Delhi, for an award of a research fellowship to R.N.D.P. The work was supported in part by a grant from the Department of Atomic Energy, Government of India.

Registry No. DL-adhb, 36207-45-1; DL-ahpp, 36207-44-0.

(48) Reference 22, p 786.
(49) Stacey, M.; Tatlow, J. C. *Advances in Fluorine Chemistry*; ed. Sharpe, A. G.; Stacey, M.; Tatlow, J. C., Butterworths, London: 1960; Vol. 1, p 166.

Contribution from the Istituto di Chimica Generale ed Inorganica, Facolta di Scienze, Universita di Parma, Viale delle Scienze, 78, 43100 Parma, Italy

Potentiometric and Spectrophotometric Study of the Proton, Cobalt(II), Nickel(II), and Copper(II) Complexes of 2-Amino-*N*,3-dihydroxybutanamide and 2-Amino-*N*-hydroxy-3-phenylpropanamide in Aqueous Solution†

Enrico Leporati

Received November 30, 1988

The equilibria and relevant stability constants of species present in aqueous solutions of cobalt(II), nickel(II), and copper(II) with DL-threonyl hydroxamic acid (2-amino-*N*,3-dihydroxybutanamide, adhb) and DL-phenylalanyl hydroxamic acid (2-amino-*N*-hydroxy-3-phenylpropanamide, ahpp) were determined by using both a potentiometric method and a spectrophotometric method in 0.5 mol dm^{-3} KCl solution at 25 °C. The protonation constants of the ligands and the formation constants of several metal complexes were calculated from potentiometric and spectrophotometric data with the aid of the SUPERQUAD and SQUAD programs, respectively. The following cumulative association constants $\beta_{pqr} = [M_pH_qL_r]/[M]^p[H]^q[L]^r$ were obtained: adhb, log β_{011} = 12.746 (1), log β_{021} = 21.614 (1), log β_{031} = 28.387 (3); Co^{II}–adhb, log β_{101} = 5.787 (16), log β_{102} = 10.299 (16), log β_{1-12} = 1.429 (36), log β_{201} = 8.807 (36); Ni^{II}–adhb, log β_{101} = 6.476 (7), log β_{102} = 13.300 (4), log β_{1-12} = 5.115 (13); Cu^{II}–adhb, log β_{102} = 19.507 (10), log β_{2-12} = 20.377 (10), log β_{1-12} = 9.918 (28); ahpp, log β_{011} = 9.013 (5), log β_{021} = 15.899 (7); Cu^{II}–ahpp, log β_{102} = 19.783, log β_{2-12} = 20.750 (39). The ligands are bound to the metal ions through the N atom of the α-amino group and the deprotonated -NHO^- group in a bidentate manner. The UV–visible studies provide important evidence for the formation of different metal(II) complexes with 2-amino-*N*,3-dihydroxybutanamide, depending on the pH. The experimental curves [$\epsilon = f(\lambda)$], deduced from refinement of absorbance data with the program SQUAD, have been resolved into precisely positioned absorption bands by Gaussian analysis using a nonlinear least-squares computer program NLIN. The resulting data for metal(II)–adhb systems have been used in weak tetragonal (CuL_2) or a square-planar (NiL_2) ligand-field models to calculate as far as possible ligand-field parameters. The solution electronic spectra can be also employed to observe the equilibria between different complexes and to estimate the coordination sphere around the metal ions. Equilibrium constants for their formation and the probable structures of the chelated compounds formed in aqueous solution are the object of discussions in terms of their possible significance to biological reactions, and their stability is compared with that of analogous chelated compounds.

Introduction

There has been a great deal of interest in recent years regarding the chemistry of hydroxamic acid derivatives due to their biological importance and analytical and industrial applications. For example, along with amino acids, hydroxamic acid derivatives have been widely investigated as inhibitors of proteolytic enzymes. Some of these compounds have showed themselves to be potent inhibitors of thermolysin,[1,2] elastase,[3] and aminopeptidases[4,5] as well as growth factors, tumor inhibitors, constituents of antibiotics, and cell division and pigments factors.[6-8] These enzymes are

† Abbreviations: aha = 2-amino-*N*-hydroxyacetamide, ahp = 2-amino-*N*-hydroxypentanamide, hasn = *N*-hydroxy-D-asparagine, ahhe = 2-amino-*N*-hydroxyhexanamide, ahpr = 2-amino-*N*-hydroxypropanamide, ahip = α-amino-*N*-hydroxy-1*H*-imidazole-4-propanamide, ahhpp = 2-amino-*N*-hydroxy-3-(*p*-hydroxyphenyl)propanamide, ahinp = α-amino-*N*-hydroxy-1*H*-indole-3-propanamide, ahpp = 2-amino-*N*-hydroxy-3-phenylpropanamide, adhp = 2-amino-*N*,3-dihydroxypropanamide.

(1) Nishino, N.; Powers, J. C. *Biochemistry* **1978**, *17*, 2846.
(2) Rasnick, D.; Powers, J. C. *Biochemistry* **1978**, *17*, 4363.
(3) Nishino, N.; Powers, J. C. *J. Biol. Chem.* **1980**, *225*, 3482.
(4) Baker, J. O.; Wilkes, S. H.; Bayliss, M. E.; Prescott, J. M. *Biochemistry* **1983**, *22*, 2098.
(5) Wilkes, S. H.; Prescott, J. M. *J. Biol. Chem.* **1983**, *258*, 13517.
(6) Dixon, N. E.; Blakely, R. L.; Zerner, B. *Can. J. Biochem.* **1980**, *58*, 1323.
(7) Neilands, J. B. *Struct. Bonding (Berlin)* **1966**, *1*, 59.
(8) Maehr, H. *Pure Appl. Chem.* **1971**, *28*, 603.

0020-1669/89/1328-3752$01.50/0

metalloproteases, and the mechanism of inhibition appears to involve chelation of metal ions at their active sites. The inhibitory effects of *N'*-hydroxy derivatives of naturally occurring amino acid amides [in this paper, these compounds are referred to by retaining the name of the aminoacyl radical and identifying the acid function involved even though systematic names would be *N*-hydroxy-α-amino ... amides] on urease of Jack bean and the rat alimentary tract were investigated.[9] Methionyl hydroxamic acid was the most powerful inhibitor among 19 α-aminoacyl hydroxamic acids. *Phenylalanyl*, seryl, alanyl, glycyl, histidyl, *threonyl*, leucyl, and arginyl hydroxamic acids followed in order of decreasing inhibitory power. The results obtained in the above-mentioned work suggest that the dissociation of an acidic (–COOH or –NHOH) or a basic ($-NH_2$) group reduces the inhibitory power of hydroxamic acids, while additional structure–activity relations show that –CONHOH group was essential for urease activity. Hydroxamic acids inhibit urease activity with strict specificity, except for aspartyl β-hydroxamic acid, which inhibits asparaginase competitively. It is also known that hydroxamic acids reveal a number of pharmacological actions including antineoplastic, antimicrobial, fungicidal, antituberculous, and antileucemic activities.[10-12] All these properties are intimately connected with iron transport phenomena in the metabolism of microorganisms.[13] More recently, interest in this class of compounds has been growing mainly due to the fact that they are capable of binding Fe(III) selectively among a number of physiologically important metal ions. Moreover, amino hydroxamic acids can be employed as indicators of biological activity with the eventual purpose to design metal–hydroxamates as suitable sources of various trace elements that are essential in animal nutrition. The hydroxamic moiety (–NHOH) is a constituent of antibiotics, antifungal agents, food additives, tumor inhibitors, and growth factors. Its derivatives are widely used in nuclear fuel processing, in frozen systems proteinases, in extractive metallurgy, and in copper corrosion inhibition. Even in the field of analytical chemistry amino hydroxamic acids have long had an important role, for example as analytical reagents for a variety of metal ions.[14] Although a lot of work has been done on their synthesis and biological and structural characterization, relatively fewer papers have appeared dealing with the solution equilibria of proton and metal complexes of hydroxamic acids, and the amount of spectrophotometric studies done on these systems is very small. In continuation of our recent efforts to understand the thermodynamic stabilities of metal complexes containing polydentate ligands and as a part of our ongoing research program, detailed potentiometric and spectrophotometric studies of several transition metal complexes of 2-amino-*N*,3-dihydroxybutanamide (adhb) and 2-amino-*N*-hydroxy-3-phenylpropanamide (ahpp) have been undertaken.

Experimental Section

Reagents. The ligands adhb and ahpp were obtained from Sigma (St. Louis, MO), and their purity was checked by potentiometric titrations. Doubly distilled and deionized water was employed and reagent grade chemicals were used without further purification. All other metal salt (chlorides, AnalaR Products) solutions were prepared and standardized by using standard analytical procedures.[15,16] All titration solutions were prepared to have a total volume of 25.0 cm^3 and thermostated at 25.0 ± 0.1 °C with a Paratherm electronic (Julabo) circulating constant-temperature water bath. The ionic strength was kept at 0.5 mol dm^{-3} with KCl. High-purity potassium chloride (Merck) was used as the supporting electrolyte. All these solutions were then raised to a final total volume of 25.0 cm^3 by adding successively to the titration vessel a known volume of adhb or ahpp solution and an exact volume of metal chloride; then, the required quantities of potassium chloride and a sufficient amount of doubly distilled water were added to make up the total volume V_0. The accurate molarity of potassium hydroxide (ca. 0.4083 mol dm^{-3}) and hydrochloric acid (0.2969 mol dm^{-3}) stock solutions were determined by conventional potentiometric titration according to Gran's method, with the use of different calculation procedures as previously described.[15-17]

Potentiometric Measurements. The equilibrium studies were performed by using a Metrohm Titroprocessor E 636 instrument. The electrode pair consisted of a Model H 268 glass electrode (Schott-Jena glass) and a Model B 343 Talamid reference electrode (Schott-Jena glass). The system was calibrated in terms of hydrogen ion concentrations before and after a series of measurements by titrations of hydrochloric acid solution at 25.0 ± 0.1 °C and I = 0.5 mol dm^{-3} (KCl) with standard carbonate-free potassium hydroxide solution, according to Gran's method,[18] by using the computer program NBAR[19] as previously reported.[20-22] The temperature was maintained at 25.0 ± 0.1 °C inside the reaction cell, and the solution was shaken by means of a mechanical stirrer. A thermostated nitrogen atmosphere, presaturated with water vapor, was maintained in the vessel throughout all titrations by blowing nitrogen over the surface of the solution. The alkalimetric titrations (dynamic and monotonous) for solutions of binary systems containing protons, copper(II), nickel(II), cobalt(II), and ligand (adhb or ahpp) were made in a similar way as described in our published works.[15-17] All the liquid-junction potentials, relative to the measurement cell, are found to be fairly small and then not significant in calculating the equilibria (pH interval used 2.547–11.903); they have been neglected in the present calculations.

Quantities of the titrant KOH were added by using a Metrohm Dosimat E 635 autoburet (total volume 5.0 cm^3).

Spectrophotometric Measurements. Absorption spectra in the ranges 410–700 ± 0.3 nm for Co^{2+}–adhb, 410–800 ± 0.3 nm for Cu^{2+}–adhb, and 360–700 ± 0.3 nm for Ni^{2+}–adhb systems were recorded on a Hitachi U-3200 spectrophotometer to the fourth decimal place with a stepping of 5.0 nm, obtaining 59, 79, and 69 absorbance values, respectively. Solutions containing ligand and metal ion, prepared and maintained under purified nitrogen with an ionic strength of 0.5 mol dm^{-3} (KCl), were scanned at a series of pH values from 3.403 to 10.660 at 25 °C by using a 10-mm cell. Potential measurements in order to obtain pH were made with the system used in the potentiometric titrations, calibrated in the same way.

Calculations. Careful attention has been paid to the calculation and critical evaluation of some parameters ($E°$, A_j, B_j, N, K_w) relating to potentiometric calibration curves, by using different mathematical methods as previously described.[20-22] Initial estimates of formation constants and the stoichiometries of possible complexes were obtained, in the case of the binary systems, from the features of the protonation and formation curves ($\bar{n}$ against pL, pL = –log [L^-]) by using GAUSS Z[23] and NBAR[19] programs. Subsequently, following our usual approach, the SUPERQUAD program[24] was employed to refine the formation constants and, on the basis of the usual numerical criteria, to select the initial sets of complexes. This last program calculates the values of the cumulative protonation and formation constants which minimize the weighted sum (U_E) of the squared residual between observed (obs) and calculated (calc) emf values (eq 1). The parameter Z is the total number of potentiometric data used in the refinement process, and w_i is the weighting factor. The equilibria reactions for the systems investigated can be expressed (charges are omitted for simplicity) by eq 2. The overall formation constant for the species $[M_pH_qL_r]$ (M = metal ion, H = proton, and L = free ligand) is defined as

$$U_E = \sum_{i=1}^{z} w_i (E_i^{obs} - E_i^{calc})^2 \quad (1)$$

$$pM + qH + rL \rightleftharpoons M_pH_qL_r \quad (2)$$

$$\beta_{pqr} = \frac{[M_pH_qL_r]}{[M]^p[H]^q[L]^r}$$

The models selected were those that gave the best statistical fit, consistent with chemical logic, to the range of titration data without giving any systematic drifts in the magnitudes of the residual (ΔE). The final choice

(9) Kobashi, K.; Takebe, S.; Terashima, N.; Hase, J. *J. Biochem. (Tokyo)* **1975**, *77*, 837.
(10) Hase, J.; Kobashi, K.; Kawaguchi, N.; Sakamoto, K. *Chem. Pharm. Bull.* **1971**, *19*, 363.
(11) Coutts, R. T. *Can. J. Pharm. Sci.* **1967**, *2*, 1.
(12) Coutts, R. T. *Can. J. Pharm. Sci.* **1967**, *2*, 27.
(13) Neilands, J. B. *J. Bacteriol.* **1976**, *126*, 823.
(14) Agrawal, Y. K. *Bull. Soc. Chim. Belg.* **1980**, *89*, 166.
(15) Leporati, E. *J. Chem. Soc., Dalton Trans.* **1986**, 2587.
(16) Leporati, E. *J. Chem. Soc., Dalton Trans.* **1987**, 435.
(17) Leporati, E. *J. Chem. Soc., Dalton Trans.* **1987**, 1409.
(18) Gran, G. *Analyst (London)* **1952**, *77*, 661.
(19) Harris, H. S.; Tobias, R. S. *Inorg. Chem.* **1969**, *8*, 2259.
(20) Leporati, E. *J. Chem. Soc., Dalton Trans.* **1985**, 1605.
(21) Leporati, E. *J. Chem. Soc., Dalton Trans.* **1986**, 199.
(22) Leporati, E. *Anal. Chim. Acta* **1985**, *170*, 287.
(23) Tobias, R. S.; Yasuda, M. *Inorg. Chem.* **1963**, *2*, 1307.
(24) Gans, P.; Sabatini, A.; Vacca, A. *J. Chem. Soc., Dalton Trans.* **1985**, 1195.

Table I. Determination of Protonation and Complex Formation Constants[a]

run	system	T_L	T_M	T_H	pH
1	H^+–adhb	0.297 428		0.892 284	4.064–11.784
2		0.260 249		0.780 749	5.581–11.903
3		0.312 299		0.936 898	5.537–11.850
4		0.282 557		0.847 670	4.154–11.781
5		0.245 378		0.736 134	4.257–11.768
6		0.327 171		0.981 512	4.242–11.896
7	Cu^{II}–adhb	0.296 792	0.152 739	0.596 724	3.244–5.377
8		0.296 792	0.101 826	0.596 724	3.279–10.44
9		0.296 792	0.050 913	0.596 724	3.36–9.85
10		0.333 891	0.101 826	0.671 315	3.256–9.894
11		0.259 693	0.101 826	0.522 134	3.264–10.342
12		0.222 594	0.050 913	0.447 543	3.41–10.181
13	Ni^{II}–adhb	0.296 792	0.147 010	0.596 724	4.961–10.497
14		0.296 792	0.073 505	0.596 724	5.081–10.240
15		0.296 792	0.036 753	0.596 724	5.203–10.470
16		0.222 594	0.073 505	0.447 543	5.165–10.613
17		0.244 854	0.066 155	0.492 297	5.145–10.432
18		0.259 693	0.110 258	0.522 134	5.031–10.589
19	Co^{II}–adhb	0.296 792	0.142 265	0.596 724	4.618–8.964
20		0.296 792	0.099 586	0.596 724	4.613–8.926
21		0.296 792	0.071 133	0.596 724	4.669–8.844
22		0.237 434	0.085 359	0.477 379	4.802–8.910
23		0.222 594	0.099 586	0.447 543	4.770–8.944
24		0.252 273	0.071 133	0.507 215	4.719–8.878
25	H^+–ahpp	0.241 995		0.563 737	2.566–10.228
26		0.215 107		0.501 100	2.591–10.906
27		0.204 352		0.476 045	2.596–10.995
28		0.225 863		0.526 154	2.638–10.043
29		0.231 240		0.538 682	2.547–10.875
30		0.209 729		0.488 572	2.562–11.147
31	Cu^{II}–ahpp	0.217 965	0.050 913	0.505 075	3.225–5.215
32		0.217 965	0.101 826	0.505 075	3.372–5.304
33		0.136 228	0.040 731	0.315 672	3.502–5.097
34		0.119 881	0.050 913	0.277 791	3.496–4.449
35		0.163 474	0.050 913	0.378 806	3.448–5.399

[a] Initial amounts of the reagents for the potentiometric titrations of 2-amino-*N*,3-dihydroxybutanamide (adhb) and 2-amino-*N*-hydroxy-3-phenylpropanamide (ahpp) with bivalent metal ions at 25 °C and I = 0.5 mol dm^{-3} (KCl) are given. T_L = mmol of ligand, T_M = mmol of metal, and T_H = mmol of hydrogen ion in the titration vessel.

Chart I. H_2L^+ with the Three Removable Protons (1–3) Indicated

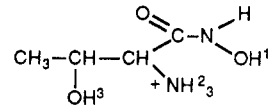

Hadhb

between combinations with similar SUPERQUAD analyses was based on graphical comparisons between calculated curves and the corresponding simulated data obtained from the HALTAFALL[25] computer program. All the calculations were carried out on the CRAY X-MP/48 and IBM 4341/10 computers of the Consorzio per la Gestione del Centro di Calcolo Elettronico Interuniversitario dell'Italia Nord Orientale, Casalecchio di Reno, Bologna, Italy, with financial support coming from the University of Parma. The compositions of the starting solutions for all potentiometric experiments are quoted in Table I. Concentrations and the experimental pH of the different solutions employed in the spectrophotometric experiments are reported in Table II. Listings of the experimental data and final computations from SUPERQUAD, GAUSS Z, NBAR, and SQUAD[26] are available on request from the author.

Results and Discussion

Protonation Equilibria. In the first place, the overall protonation constants of the ligands and the initial amounts (mmol) of reagents (T_L, T_H) were determined at the same time through the refinement of several sets of potentiometric data by SUPERQUAD without introducing into the calculations the liquid-junction potentials (A_j and B_j) as shown in already published papers.[20-22] At the end

(25) Ingri, N.; Kakalowicz, W.; Sillén, L. G.; Warnqvist, B. *Talanta* **1967**, *14*, 1261.
(26) Leggett, D. J.; McBryde, W. A. E. *Anal. Chem.* **1975**, *47*, 1065.

Table II. Initial Concentration (C/mol dm^{-3}), Standard Deviation of Absorbance (SDA),[a] and the Measured pH of the Solutions Employed in the Spectrophotometric Experiments

run	system	C_L	C_M	pH	SDA
1	Cu^{2+}–adhb	1.0450×10^{-2}	5.3780×10^{-3}	3.570	1.418×10^{-2}
2		1.0351×10^{-2}	5.3272×10^{-3}	4.133	1.229×10^{-2}
3		1.1095×10^{-2}	3.8066×10^{-3}	10.491	5.475×10^{-3}
4		1.0972×10^{-2}	3.7644×10^{-3}	8.898	3.049×10^{-3}
5		1.0891×10^{-2}	3.7367×10^{-3}	6.946	4.150×10^{-3}
6		1.0844×10^{-2}	3.7204×10^{-3}	5.854	1.397×10^{-2}
7		1.0804×10^{-2}	3.7068×10^{-3}	5.213	8.292×10^{-3}
8		1.0753×10^{-2}	3.6894×10^{-3}	4.855	1.014×10^{-2}
9		1.0695×10^{-2}	3.6694×10^{-3}	4.040	4.345×10^{-3}
10		1.0619×10^{-2}	3.6432×10^{-3}	3.560	7.051×10^{-3}
11		1.1189×10^{-2}	1.9194×10^{-3}	9.852	8.129×10^{-3}
12		1.1105×10^{-2}	1.9051×10^{-3}	9.025	4.125×10^{-3}
13		1.0982×10^{-2}	1.8839×10^{-3}	7.634	1.106×10^{-2}
14		1.0842×10^{-2}	1.8598×10^{-3}	5.830	7.766×10^{-3}
15		1.0794×10^{-2}	1.8517×10^{-3}	4.848	1.151×10^{-2}
16		1.0716×10^{-2}	1.8383×10^{-3}	3.741	1.062×10^{-2}
17		1.2459×10^{-2}	3.7995×10^{-3}	9.850	5.665×10^{-3}
18		1.2321×10^{-2}	3.7574×10^{-3}	8.516	4.368×10^{-3}
19		1.2186×10^{-2}	3.7163×10^{-3}	6.232	6.908×10^{-3}
20		1.2119×10^{-2}	3.6960×10^{-3}	5.183	8.047×10^{-3}
21		1.2076×10^{-2}	3.6827×10^{-3}	4.924	5.527×10^{-3}
22		1.1989×10^{-2}	3.6562×10^{-3}	4.043	4.938×10^{-3}
23		1.1925×10^{-2}	3.6366×10^{-3}	3.616	6.305×10^{-3}
24		1.1840×10^{-2}	3.6108×10^{-3}	3.403	1.041×10^{-2}
25		0.9791×10^{-2}	3.8389×10^{-3}	10.293	9.208×10^{-3}
26		0.9677×10^{-2}	3.7945×10^{-3}	8.055	3.730×10^{-3}
27		0.9606×10^{-2}	3.7665×10^{-3}	5.416	8.003×10^{-3}
28		0.9500×10^{-2}	3.7251×10^{-3}	4.140	5.981×10^{-3}
29		0.9466×10^{-2}	3.7115×10^{-3}	3.753	6.438×10^{-3}
30	Ni^{2+}–adhb	1.1043×10^{-2}	5.4700×10^{-3}	10.560	7.087×10^{-3}
31		1.0922×10^{-2}	5.4098×10^{-3}	7.659	5.612×10^{-3}
32		1.0842×10^{-2}	5.3702×10^{-3}	6.298	4.340×10^{-3}
33		1.0763×10^{-2}	5.3313×10^{-3}	5.908	3.695×10^{-3}
34		1.0647×10^{-2}	5.2739×10^{-3}	5.610	3.960×10^{-3}
35		1.1126×10^{-2}	2.7556×10^{-3}	10.443	6.237×10^{-3}
36		1.0978×10^{-2}	2.7189×10^{-3}	8.357	5.843×10^{-3}
37		1.0854×10^{-2}	2.6881×10^{-3}	6.802	6.481×10^{-3}
38		1.0775×10^{-2}	2.6685×10^{-3}	5.974	3.493×10^{-3}
39		1.0697×10^{-2}	2.6493×10^{-3}	5.661	5.366×10^{-3}
40		1.1158×10^{-2}	1.3817×10^{-3}	10.616	2.774×10^{-3}
41		8.4476×10^{-3}	2.7896×10^{-3}	10.660	6.115×10^{-3}
42		8.3525×10^{-3}	2.7582×10^{-3}	8.119	3.014×10^{-3}
43		8.2903×10^{-3}	2.7376×10^{-3}	6.467	3.694×10^{-3}
44		8.2442×10^{-3}	2.7224×10^{-3}	5.962	6.901×10^{-3}

[a] SDA = $[\sum_{K=1}^{NBA} [A_o(K) - A_c(K)]^2 w_K/(NBA - NCV)]^{1/2}$ where $A_o(K)$ and $A_c(K)$ are the observed and calculated absorbance value at the Kth wavelength, NBA = number of wavelengths, and NCV = number of constants to be varied; w_K = is the weighting factor.

Chart II. H_2L^+ with the Two Removable Protons (1 and 2) Indicated

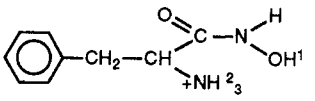

Hahpp

of this refinement the variances (σ^2) in the quantities T_L and T_H with respect to the initial values were 4.5841×10^{-7} and 1.7187×10^{-6} for adhb and 2.7867×10^{-7} and 2.5645×10^{-6} for ahpp, respectively. The refined protonation and formation constants (log β_{pqr}) for the two ligands are given in Table III. The adhb ligand (Hadhb = H_2L^+; Chart I) has three protonation centers, the terminal hydroxamate moiety (–NHO^-) (H^1; Chart I), the α-amino group (H^2; Chart I), and the alcoholate group (H^3; Chart I), while the ahpp ligand (Hahpp = H_2L^+; Chart II) can only liberate two protons, one from the OH group of the hydroxamic moiety (–NHOH) (H^1; Chart II) and one from the protonated amino group (H^2; Chart II). The ionic product of water (pK_w = 13.719 (1)) was obtained as previously described.[15-17] By analogy with the known ones of some aliphatic hydroxy derivatives the protonation constant of the alcoholate (adhb) was approximately determined by potentiometric method because of its high basicity (for log K_n^H see Table III). Therefore, GAUSS Z was employed to refine protonation constants of the two ligands,

Table III. Cumulative and Stepwise Protonation Complex Formation Constants of 2-Amino-*N*,3-dihydroxybutanamide (adhb) and 2-Amino-*N*-hydroxy-3-phenylpropanamide (ahpp) at 25 °C and I = 0.5 mol dm^{-3} (KCl)

	adhb					ahpp		
	SUPERQUAD				GAUSS Z	SUPERQUAD		GAUSS Z
	H^+	Co^{2+}	Ni^{2+}	Cu^{2+}	H^+	H^+	Cu^{2+}	H^+
$\log \beta_{011}$	12.746 (10)				12.741 (23)	9.013 (5)		9.013 (2)
$\log \beta_{021}$	21.614 (1)				21.606 (1)	15.899 (7)		15.900 (3)
$\log \beta_{031}$	28.387 (3)				28.375 (1)			
$\log K_2^{H\,a}$	8.868 (1)^b				8.865 (1)	6.886 (6)		6.887 (3)
$\log K_3^H$	6.773 (2)				6.769 (1)			
$\log \beta_{101}$		5.787 (16)	6.476 (7)					
$\log \beta_{102}$		10.299 (16)	13.300 (4)	19.507 (10)			19.783	
$\log \beta_{2-12}$				20.377 (10)			20.750 (39)	
$\log \beta_{1-12}$		1.429 (36)	5.115 (13)	9.918 (28)				
$\log \beta_{201}$		8.807 (36)						
$\log K_2$		4.512 (16)	6.824 (6)					
Z^c	267	252	364	289	267	204	76	204
U	2.836 × 10	1.017 × 10^3	1.760 × 10^2	3.610 × 10^2	4.715 × 10^{-3} ^{f}	8.697 × 10	9.301 × 10^2	1.168 × 10^{-2} ^{f}
$\chi^{2\,d}$	12.52	24.57	9.63	11.16		12.47	17.26	
σ^e	0.33	2.02	0.71	1.48	1.772 × 10^{-5} ^{g}	0.68	3.59	5.781 × 10^{-5} ^{g}
R^h					0.2			0.6

$^a \log K_n = \log \beta_{0n1} - \log \beta_{0(n-1)1}$. $^b \sigma(\log K_n) = \{[\sigma^2(\log \beta_{0n1}) + \sigma^2(\log \beta_{0(n-1)1})/2]\}^{1/2}$. ^{c} Total number of experimental data points used in the refinement. ^{d} Observed χ^2; the calculated value (6, 0.95) should be 12.6, where 6 is the number of degrees of freedom and 0.95 is the confidence coefficient in the χ^2 distribution. $^e \sigma = [\sum_{i=1}^{Z} w_i(E_i^{obs} - E_i^{calc})^2/(Z - m)],^{1/2}$ where m is the number of parameters to be refined. $^f U = \sum_{i=1}^{Z}(\bar{n}_i^{calc} - \bar{n}_i^{obs})^2$, where $\bar{n}_i$ is the observed (obs) or calculated (calc) average number of hydrogen ions bound to each central ligand molecule. $^g \sigma^2 = \sum_{i=1}^{Z}(\bar{n}_i^{calc} - \bar{n}_i^{obs})^2/(Z - m)$. $^h R = [\sum_{i=1}^{Z}(\bar{n}_i^{obs} - \bar{n}_i^{calc})^2/\sum_{i=1}^{Z}(\bar{n}_i^{obs})^2]^{1/2}$ 100.0%.

starting from the same experimental data. All the protonation constants calculated by both computer methods (Table III) agree closely, and the standard deviations of the refined quantities were very small. The presence of the α-amino group in adhb and ahpp increases the acidic character of the OH group of the hydroxamic moiety (–NHOH) in comparison with that of the related compounds CH_3–CH(OH)–CH_2–CONHOH (log K_2^H = 9.23) and C_6H_5–CH_2–CH_2–CONHOH (log β_{011} = 9.38). This increase of acidic character (decrease in protonation constant of the –NHOH group) in all amino hydroxamic acids investigated takes place in the order hasn[27] < aha[15] < ahhe[28] < ahp[15] < ahpr[29] < ahip[16] < ahinp[28] < ahhpp[17] < ahpp < adhp[30] < adhb. Likewise, the replacement of a –NHOH group for the carboxyl OH group in amino hydroxamic acids examined lowers remarkably the protonation constant of the corresponding α-amino acids due to the electron-withdrawing effect of the –NHOH group. This increase in the acidic character of the $-NH_3^+$ group follows the order hasn[27] < ahhe[28] < ahpr[29] < ahp[15] < aha[15] < ahinp[28] < ahpp < ahip[16] < ahhpp[17] < adhp[30] < adhb.

Metal(II) Complex Equilibria. Attempts were made to fit a large number of different models to the experimental data, and the model selected gave the best statistical fit over the data available. The neutral ligand is referred to as HL for both adhb and ahpp. The formation constants obtained from the present work are shown in Table III. Where values for a particular species are not included in Table III, it means that the species was apparently absent or contributed an insignificant amount to the equilibrium (and hence had an insignificant effect on the statistical fit of the data). Since in the complex formation the adhb ligand shows a behavior very similar to that of the already investigated amino hydroxamic acids[15-17] without the OH^- group, it is possible to suppose that the proton residing on the alcoholic group (Chart I) is not ionized when the complex formation equilibria take place. Consequently, in the refinement process of the species complexed, the H_2L^+ ligand with only two dissociable groups (–NHOH, NH_3^+) has been considered, introducing into the calculations log β_{011} (8.868) and log β_{021} (15.641) as constants. The refinement converged satisfactorily when the only species present for adhb were $[Cu_2(OH)L_2]^+$, $[CuL_2]$, and $[Cu(OH)L_2]^-$ for Cu^{2+}; $[NiL]^+$, $[NiL_2]$, and $[Ni(OH)L_2]^-$ for Ni^{2+}; and $[Co_2L]^{3+}$, $[CoL]^+$, $[CoL_2]$, and $[Co(OH)L_2]^-$ for Co^{2+}. The most consistent set of

Chart III

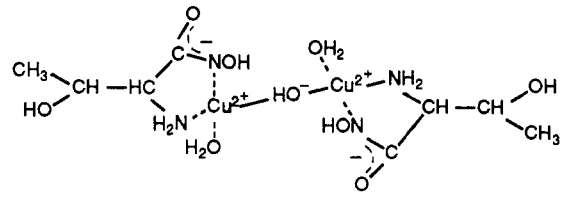

complexes found for ahpp, together with their respective formation constants shown in Table III, was $[Cu_2(OH)L_2]^+$ and $[CuL_2]$ only. Equilibria between Co^{2+} and Ni^{2+} ions and ahpp cannot be studied because at the already acid pH precipitation occurs in the titration vessel. The inclusion of further possible species for all the systems examined had no significant effect on the statistics of the fit, the complexes contributing to the general species distribution by a negligible amount. A typical species distribution graph for a metal(II)–adhb mixture is shown in Figure 1. The most important details arising from this study are thermodynamic conclusions, which suggest the structures of the complexes present in aqueous solution. Spectral investigations of structures perceive only those aspects of the structure that are involved in electronic transitions. On the other hand, the spectrophotometric characteristics and the numerical interpretation of the most stable complex (CuL_2 or NiL_2) reflect all bond strengths, ring strains, the coordination sphere around the metal ions, and configurations. The species distribution curves (Figure 1) show that complexation begins at low pH values; ca. 3.25 for $[Cu_2(OH)L_2]^+$ species and ca. 5.0 for Co^{2+} and Ni^{2+} with formation of the mononuclear complex $[ML]^+$ corresponding to the release of two protons per metal respectively; the complex $[ML]^+$ accounts for a maximum concentration of 52.0% of the total cobalt at pH 6.6 and 26.0% of the total nickel at pH 5.6. In the case of the Co^{2+}–adhb system, the $[Co_2L]^{3+}$ dinuclear species has been also found, which reaches a peak of 46.0% at pH 5.9; in the presence of Cu^{2+} the formation in strongly acidic media of hydrolyzed dinuclear species $[Cu_2(OH)L_2]^+$ has been observed, which reaches a maximum concentration of 91.8% total copper at pH 4.15. The studies of the equilibria existing between Cu(II) ion and other analogous aminoalkanohydroxamic acids[29,31] have indicated the presence of an OH^- group in the dinuclear species.[31] This one OH^- ion acts as a bridge group (Chart III) and originates from the displacement of a proton from a coordinated water molecule in the $[CuL]^+$ units to give the

(27) Leporati, E. *J. Chem. Soc., Dalton Trans.*, in press.
(28) Leporati, E. *J. Chem. Soc., Dalton Trans.* **1987**, 421.
(29) Kurzak, B.; Kurzak, K.; Jezierska, J. *Inorg. Chim. Acta* **1986**, *125*, 77.
(30) Leporati, E. *Gazz. Chim. Ital.* **1989**, *119*, 183.
(31) Paniago, E. B.; Carvalho, S. *Inorg. Chim. Acta* **1984**, *92*, 253.

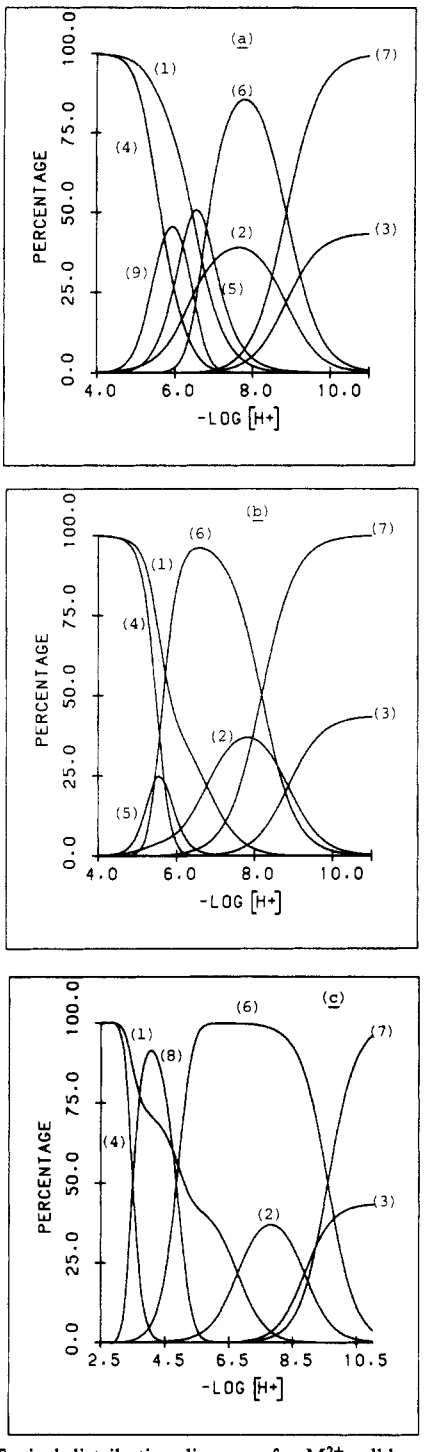

Figure 1. Typical distribution diagrams for M^{2+}–adhb systems. The percentage of each species has been calculated from the data of a hypothetical solution of metal ions (0.0031 mol dm^{-3}) and adhb (0.011 mol dm^{-3}) by the HALTAFALL program[25] and plotted with a Calcomp 936 plotter. The concentrations of the species not containing metal were calculated as percentages of the total ligand; those containing metal were calculated as percentages of the total metal: (a) Co^{2+}–adhb; (b) Ni^{2+}–adhb; (c) Cu^{2+}–adhb; (1) H_2L^+; (2) HL; (3) L^-; (4) M^{2+}; (5) $[ML]^+$; (6) $[ML_2]$; (7) $[M(OH)L_2]^-$; (8) $[Cu_2(OH)L_2]^+$; (9) $[Co_2L]^{3+}$.

complex $[Cu_2(OH)L_2]^+$. It is interesting to note that previous authors[29,31] concluded that the dimer $[Cu_2(OH)L_2]^+$ was the major species in equilibrium with mononuclear complex $[CuL]^+$ (minor species not more than ca. 18–25% of the total copper content at pH < 5.0). In the present work, all our attempts to retain such a simplex species $[CuL]^+$ in our minimizations failed, and from all statistical evidence, we obtained entirely acceptable fits without its inclusion. It is difficult to suggest an explanation for such contradictory results, unless they are a result of the trial models

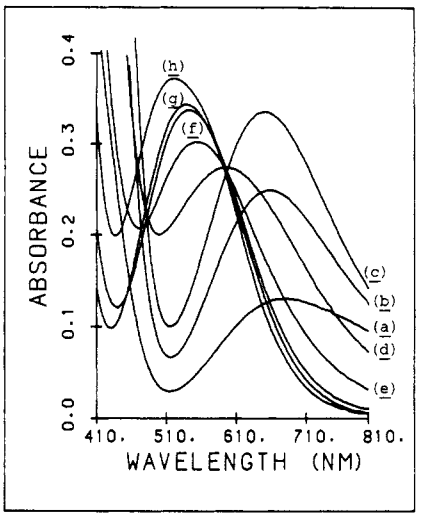

Figure 2. Plots of experimental absorbance data versus wavelength for solutions [runs 24 (a), 23 (b), 22 (c), 21 (d), 20 (e), 19 (f), 18 (g), and 17 (h) from table II] of the Cu^{2+}–adhb system at 25 °C obtained by using the program VISION with a Calcomp 936 plotter.

and minimization technique employed. Nevertheless a probable explanation of this behavior may lie in the decreasing basicity of the functional groups ($-NHO^-$, $-NH_2$) under the influence of the decreased bonding interactions to give the structure $[CuL]^+$ as well as steric factors. Typical absorption spectra for the Cu^{2+}–adhb system are shown in Figure 2 for the range pH 3.403–9.852. They consist of two bands at 521–553 (Figure 2d–h) and 650.6 (Figure 2c) nm. The absorption spectra of the Cu(II)–threonyl hydroxamic acid system exhibit, in general, approximately the same changes with increasing pH to those stated for the Cu–alkanohydroxamic acid (alkanohydroxamic acid = aha,[15,31] adhp,[30] ahpr[29]) system. Some differences are observed in the energy of the characteristic absorption maxima. At low pH the absorption presents a broad spectrum near the infrared region, its maximum shifting progressively into the visible region as the pH is increased. At pH 4.043, the maximum occurring at 651 nm (Figure 2c) corresponds to the greatest concentration of the hydrolyzed dimeric complex (Figure 1c), while a maximum at 553 nm (Figure 2d) is reached at pH 5.183, which corresponds to the maximum in the concentration (86%) of the complex species $[CuL_2]$ at about this same pH (Figure 1c).

According to Narain and Shulka[32] the position of the absorption maxima for Cu(II) complexes in aqueous solution depends on the number of Cu–N bonds. The maximum in the range 620–650 nm is typical for Cu(II) coordinated by two nitrogen atoms of the amino or amido groups of the α-amino acids or peptides, respectively. Since the hydrolyzed dinuclear species $[Cu_2(OH)L_2]^+$ exhibits λ_{max} at 650.6 nm, it is possible to conclude that every copper ion is coordinated by two nitrogen atoms of adhb. In the same way, the $[CuL_2]$ complex with dipeptides show an absorption maximum at 540–560 nm. Therefore, the appearance of the absorption peak at 553 nm of $[CuL_2]$ with adhb suggests the coordination of one copper ion by two ligands, forming two five-membered chelate rings and four Cu–N bonds with participation of the two nitrogens of the α-amino and deprotonated $-NHO^-$ groups. According to Billo,[33] the ligand-field contribution of each N(amino) is equal to 4530 cm^{-1}, which means that the contribution of the two nitrogens of the hydroxamate moiety in the $[CuL_2]$ complex formation with λ_{max} = 18 083 cm^{-1} corresponds to: (18 083 − 9060)/2 = 4512 cm^{-1}. For the hydrolyzed dinuclear complex $[Cu_2(OH)L_2]^+$, with λ_{max} = 651 nm, if we suppose coordination of one threonyl hydroxamate group to each copper ion via the nitrogens of the α-amino and hydroxamate groups, this would result in a contribution of 9042 cm^{-1} to the energy of the d–d transition. The two remaining groups would

(32) Narain, G.; Shulka, P. *Z. Anorg. Allg. Chem.* **1966**, *342*, 221.
(33) Billo, E. J. *Inorg. Nucl. Chem. Lett.* **1974**, *10*, 613.

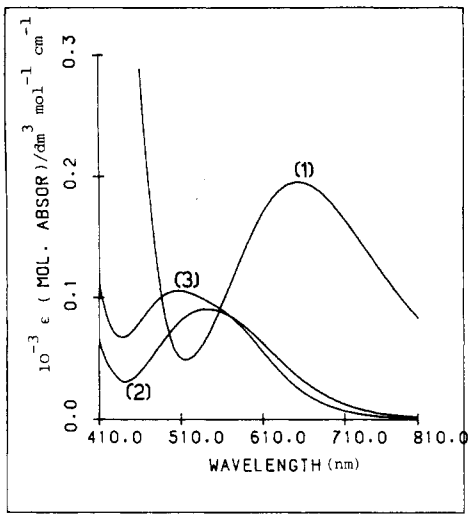

Figure 3. Plots of molar absorption coefficients (ϵ) of the three complexed species of the Cu^{2+}–adhb system at 25 °C obtained by use of the program SQUAD with a Calcomp 936 plotter: $\epsilon_{[Cu_2(OH)L_2]^+}$ (1); $\epsilon_{[CuL_2]}$ (2); $\epsilon_{[Cu(OH)L_2]^-}$ (3).

have to contribute ca. 3159 cm^{-1} each, in order to arrive at the observed λ_{max} (15 361 cm^{-1}) for the complex $[Cu_2(OH)L_2]$. This value agrees well with the predicted contribution of OH^- or H_2O groups, which is 3010 cm^{-1}. The fourth position in each copper ion is occupied equatorially by an H_2O molecule as shown in Chart III. As the pH increases further, above pH 8.0, a new shift in the spectrum is observed with a maximum occurring at 521 nm (Figure 2h). This coincides with the formation of the complex $[Cu(OH)L_2]^-$ shown in Figure 1c. A distinctive isosbestic point appears at 595 nm (Figure 2c–h). This corresponds to an equilibrium between the species $[Cu_2(OH)L_2]^+$ and $[CuL_2]$, which are predominant from pH 2.8 to 8.0, according to Figure 1c. When the pH is increased from 3.403 to 4.043 (Figure 2) small hypsochromic and high hyperchromic shifts (651–683 nm) are observed (intense green color); as the pH increases above 4.043, a simultaneous decrease in the absorption (hypochromic effect) occurs with a maximum at 651 nm and an increase in the absorption (hyperchromic effect) with a maximum at 521 nm (change of color from intense green to purple in acid media, while for pH > 8.0 the color changes from purple to reddish purple). The molar absorption coefficients ϵ_{pqr} in the range 410–800 nm for the Cu^{2+}–adhb system together with the formation constants of complexes were refined by handling the specific set of absorbance data (Table II, 29 solutions, 79 wavelengths, 2291 points) by using the SQUAD program (Figure 3). The sum of deviation squares and the standard deviation in the absorbance data of 29 solutions and 79 wavelengths was 0.1302 and 7.542×10^{-3}, respectively, meaning that the fit of the calculated spectra to the observed ones was very good. In order to interpret the CuL_2 spectrum, it is already known that electronic spectra for most octahedral and pseudooctahedral complexes of Cu(II) can be explained by the doublet term system displaying one (in the case of octahedral) or more absorption bands (e.g. three for tetragonal). The theoretical energy level diagram for a d^9 metal ion configuration[34] in O_h and D_{4h} symmetry, shown in Figure 4, indicates that as many as three doublet–doublet transitions may be observed in the electronic spectra of complexes with D_{4h} symmetry. Experimental spectra for such compounds rarely display more than two absorption bands. In some cases, however, all three absorption bands can be detected.[35] At this point, a careful and detailed Gaussian analysis of the experimental spectrum of $[CuL_2(H_2O)_2]$ (Figure 3) was carried out by using a NLIN computer program;[46] in particular, the parameters of the components bands and related maxima positions were carefully determined. This program is

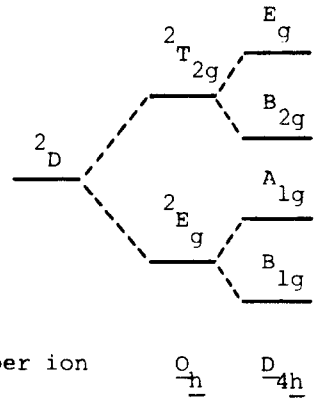

Figure 4. Splitting of the d^9 ^2D term in O_h and D_{4h} (elongated along the z axis) ligand fields (not to scale).

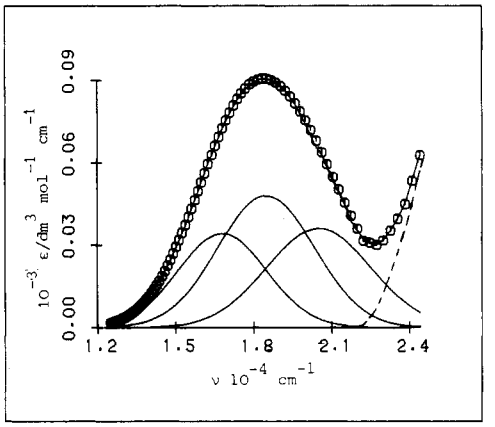

Figure 5. Absorption spectra of $[CuL_2(H_2O)_2]$: experimental (symbol) and calculated (line); (—) composite bands; (- -) unassigned band.

based on the nonlinear Gauss–Newton least-squares method. It is well-known that any curve reported in Figure 3 may be considered to be the sum of an infinite number of Gaussian components. However, it is possible to assume that a unique fitting between a wide number of different models could be obtained if the relative symmetry is taken into account. Since a realistic model is desired, it needs to apply to a possible reduction in the symmetry of the system. The possible effective symmetry of the investigated system is the following: O_h (one-component band) and D_{4h} (three-component bands). Most of the copper(II) complexes, which are usually green or blue, are tetragonally distorted with four short metal–ligand bonds in one plane (xy) and two longer metal–H_2O bonds lying along the z axis above and below this plane; then, the assumption of D_{4h} symmetry may be suitable to explain the spectral band locations. In fact, the further reduction in symmetry should theoretically involve additional splittings and joining them into a broadening band, while the experimental curve resolved into precisely positioned absorption bands by Gaussian analysis allowed D_{4h} symmetry, obtaining in such a way a best fit in terms of the relative standard deviation (0.64%) calculated from observed values. Finally, the assignments and calculated maxima positions of the components bands (Figure 5 and Table IV) are based on the following assumptions: the effective symmetry about the copper ion is D_{4h}, and the ligand-field model proposed is adequate to derive the spectral parameters. In this case, the B_{1g} term will be the ground state and three spin-allowed transitions from the $^2B_{1g}$ state to the other doublet states are to be expected. The relative energy order of these transitions ($^2A_{1g} < {}^2B_{2g} < E_g$) will depend on the expanse of the axial metal–H_2O interaction, and their energies in terms of parameters D_q, D_s, and D_t have been taken from the following expressions:[36]

$$\nu_1 = E(B_{1g} \rightarrow A_{1g}) = -4D_s - 5D_t$$

$$\nu_2 = E(B_{1g} \rightarrow B_{2g}) = 10D_q$$

$$\nu_3 = E(B_{1g} \rightarrow E_g) = 10D_q - 3D_s + 5D_t$$

(34) Ballhausen, C. J. *Introduction to Ligand Field Theory*; McGraw-Hill: New York, 1962.
(35) Oelkrug, D. *Struct. Bonding (Berlin)* **1971**, *9*, 1.

Table IV. Parameters (ϵ/dm^3 mol^{-1} cm^{-1}, ν/cm^{-1}, and $\Delta\nu$/cm^{-1}) of the Component Bands Obtained from Gaussian Analysis of the Absorption Spectra of $[CuL_2(H_2O)_2]$ and $[NiL_2(H_2O)_2]$, Respectively (L = DL-Threonyl Hydroxamate)[a]

assignt	ϵ	ν	$\Delta\nu$	f
		$[CuL_2(H_2O)_2]$		
$^2B_{1g} \rightarrow {}^2A_{1g}$	34.257	16800.5	4001.2	6.3052×10^{-4}
	53.711[b]	16800.2	4001.1	9.886×10^{-4}
	33.585[c]	16799.2	4147.8	6.404×10^{-4}
$^2B_{1g} \rightarrow {}^2B_{2g}$	48.002	18501.4	4374.6	9.6595×10^{-4}
	80.932[b]	18500.2	4374.9	1.629×10^{-3}
	48.113[c]	18824.0	4191.8	9.272×10^{-4}
$^2B_{1g} \rightarrow {}^2E_g$	36.102	20500.1	4705.8	7.8149×10^{-4}
	48.459[b]	20499.2	4706.1	1.049×10^{-3}
	29.558[c]	20517.7	5066.8	6.855×10^{-4}
		$[NiL_2(H_2O)_2]$		
$^1A_{1g} \rightarrow {}^1B_{1g}$	55.455	19819.7	3773.8	9.6267×10^{-4}
	53.982[d]	19779.8	3818.7	9.4825×10^{-4}
$^1A_{1g} \rightarrow {}^1A_{2g}$	58.200	23900.1	5187.6	1.3888×10^{-3}
	56.200[d]	23892.8	5187.1	1.3410×10^{-3}

[a] RSD (relative standard deviation) of Cu^{2+}–adhb system = 0.64%. Region of spectrum: 14286–27780 cm^{-1} and 12500–24390 cm^{-1} for Ni^{2+} and Cu^{2+}, respectively. [b] Cu^{2+}–adhp system. [c] Cu^{2+}–ahpr system. [d] Ni^{2+}–adhp.

From the maxima positions of the components bands (Table IV), the ligand-field parameters D_q, D_s, and D_t were deduced

$$D_q = \nu_2/10 = 1850.1 \text{ cm}^{-1}$$

$$D_s = 1/7(\nu_2 - \nu_1 - \nu_3) = -2685.8 \text{ cm}^{-1}$$

$$D_t = 1/35[4(\nu_3 - \nu_2) - 3\nu_1] = -1211.6 \text{ cm}^{-1}$$

Table IV summarizes the results of spectra resolution, parameters of the components bands, their oscillator strength values and relative standard deviation for Cu^{2+}–adhb, Ni^{2+}–adhb, and other analogous systems, respectively. From the results obtained, it is possible to verify an excellent agreement between the parameters calculated (ν, ϵ, f, $\Delta\nu$) for the different systems, meaning that a similar behavior (thermodynamic stability, structure, configuration, all bond strengths, coordination sphere) takes place through the CuL_2 complex formation. The small differences observed in the values (D_q and ϵ) could be due to various factors: D_q (inversely proportional to the fifth power of the metal–ligand distance) is very sensitive to changes in the metal–ligand distance; the metal–ligand bonds will be vibrating so that the internuclear distance is constantly fluctuating. Thus the slightly larger crystal-field parameter D_q for the Cu^{2+}–ahpr system reflects, in addition to the electrostatic interaction between metal ion and ligand, the covalent σ and π capability of the ligand, while the increment in the molar intensity (ϵ) of the components bands for the Cu^{2+}–adhp system involves a change from centrosymmetric molecules to weakly acentric molecules. The molar absorption coefficient ϵ_{pqr} in the range 360–700 nm for Ni^{2+}–adhb complexes were refined as previously described, and the sum of the squared residual between observed and calculated absorbance values (1035 experimental points) by using 15 solutions (Table II) and 69 wavelengths was 2.689×10^{-2} (the standard deviation in the absorbance data was 5.102×10^{-3}). Gaussian analysis was performed on the electronic spectrum of $[NiL_2(H_2O)_2]$ deduced from SQUAD by using an NLIN computer program. Nickel(II) readily forms planar complexes with saturated amines that sterically hinder axial ligation. In the Ni(II) complexes of glycyl hydroxamic acid,[31] a N,N-coordination was found for $[NiL_2]$ and $[Ni(OH)L_2]$, respectively. For these Ni(II) complexes in the solid state, a square-planar coordination was found, having *trans*-(NiL_2)[37] and *cis*-$[Ni(OH)L_2]$[38] configurations. Square-planar

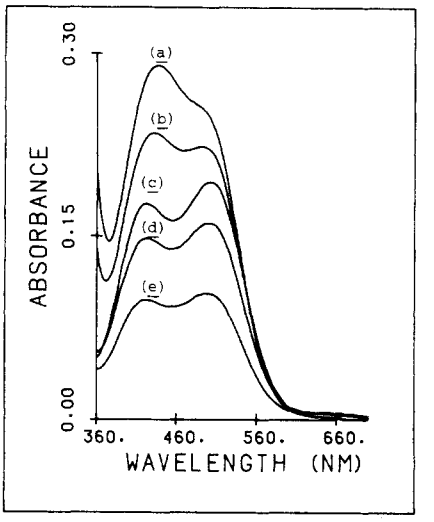

Figure 6. Plots of experimental absorbance data versus wavelength for solutions [runs 35 (a), 36 (b), 37 (c), 38 (d), and 39 (e) from Table II] of the Ni^{2+}–adhb system at 25 °C obtained by using the program VISION with a Calcomp 936 plotter.

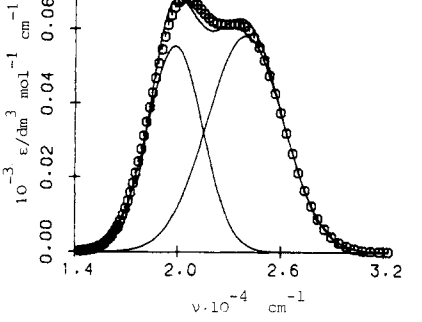

Figure 7. Absorption spectra of $[NiL_2(H_2O)]$: experimental (symbol) and calculated (line); (—) composite bands.

derivatives of nickel(II) are commonly orange or red. The d–d spectra of nickel(II) consist of a single broad asymmetric peak in the 20000–24000-cm^{-1} region that is well separated from the charge-transfer bands. The majority of these complexes exhibit a strong absorption band (ϵ = 50–500 dm^3 cm^{-1} mol^{-1}) in the visible region between 15000 and 25000 cm^{-1} and, in many cases, a second more intense band between 23000 and 30000 cm^{-1}. Typical absorption spectra for the Ni^{2+}–adhb system are reported in Figure 6 for the range pH 5.661–10.443.

The spectrum of $[NiL_2(H_2O)_2]$ could be satisfactorily resolved into three Gaussian components as would be expected for complexes of D_{4h} symmetry with no ligands coordinated along the z axis. There is considerable evidence that such Gaussian components can be considered to at least semiquantitatively represent the d–d single-electron spin-allowed–spin-allowed transitions. Then two Gaussian fits were attempted and found to be satisfactory. Figure 7 shows the experimental and calculated spectrum of $[NiL_2(H_2O)_2]$ and the component bands (full lines) obtained from spectral resolution. In a nickel complex of this kind, the $^1A_{1g}$ will be the ground state and two component bands may be tentatively assigned as ν_2 = 19820 cm^{-1} ($^1A_{1g} \rightarrow {}^1B_{1g}$) and ν_3 = 23900 cm^{-1} ($^1A_{1g} \rightarrow {}^1A_{2g}$) transitions in square-planar symmetry by comparison with observed spectra of Ni(II) complexes of confirmed square-planar configuration.[30,36,39] The only other transition expected in this region for a low-spin nickel(II) complex of D_{4h} symmetry lying below 28000 cm^{-1} ($^1A_{1g} \rightarrow {}^1E_g$) is probably a

(36) Lever, A. P. B. *Inorganic Electronic Spectroscopy*; Elsevier: New York, 1968; pp 334–335.
(37) Brown, D. A.; Roche, A. L.; Pakkanen, T. A.; Pakkanen, T. T.; Smolander, K. *J. Chem. Soc., Chem. Commun.* **1982**, 676.
(38) Julien-Pouzol, M.; Jaulmes, S.; Laruelle, P.; Carvalho, S.; Paniago, E. B. *Acta Crystallogr., Sect. C* **1985**, *41*, 712.
(39) Brown, A. D.; Roche, A. L. *Inorg. Chem.* **1983**, *22*, 2199.

charge-transfer band, not observed experimentally. Nevertheless the problem is further complicated in that the position of the a_{1g} (d_{z^2}) level depends critically upon whether the molecule is truly square planar with no near neighbors along the z axis or whether it is tetragonal with weak interactions along the z axis. Since the 1:2 nickel complex, according to X-ray data,[37,38] is N,N-coordinated forming five-membered rings, we could suggest a similar coordination for the ML species via the N atom of the amino group and the nitrogen atom of the deprotonated $-NHO^-$ group, as previously reported for nickel complexes of glycyl hydroxamic acid (aha)[15,39] and seryl hydroxamic acid (adhp).[30] The NiL_2 complex being square planar, the small difference in log K for NiL and NiL_2 species [$\Delta \log K$ (6.824 - 6.476) = 0.348] could be explained if we considered that it corresponds to an octahedral (NiL) to square-planar (NiL_2) transformation. In addition, the logarithm of the second stepwise formation constant (log K_2) for the Ni^{2+}-adhb system is appreciably greater than that of the first, log β_{101}. This is contrary to earlier findings[40-43] using a method of calculation based on the erroneous assumption that the formation of NiL is effectively complete before NiL_2 begins to be formed. The explanation of this behavior may lie in the ability of Ni^{2+} to form square-planar complexes; when a second ligand is bonding facially in a bidentate manner, the two five-membered chelate rings in the complex [NiL_2] are much more stable than one five-membered ring in the [NiL] species. In conclusion the X-ray crystal structures of two complexes of nickel(II)[37,38] and one of copper(II)[44] containing two glycyl hydroxamate anions (L^- = $H_2N-CH_2-CONHO^-$) provide evidence of coordination by the nitrogen amino and the nitrogen of the hydroxamate moiety for adhb and ahpp, respectively. Additional evidence for this type of coordination, which persists in solution, was given by potentiometric and spectrophotometric studies on nickel(II)[39,45] and copper(II).[31] We conclude therefore that M(II)adhb and M(II)-ahpp systems can probably satisfy different criteria for the biological activities and the analytical role proposed, giving a strong indication for the complexes investigated as being suitable sources of metal ions as trace elements that are essential in animal nutrition. Our results show clearly that, at physiological pH values, the assumption of an uncoordinated α-amino group in the M(II)-adhb and M(II)-ahpp systems is probably incorrect since the major species in this pH range is ML_2, which involves coordination of the α-amino group and hydroxamate $-NHO^-$ moiety.

Acknowledgment. Financial support in part by the Ministero della Pubblica Istruzione, Rome, and by the National Research Council of Italy (CNR) is gratefully acknowledged. I am greatly indebted to Professor P. Gans, Professor A. Vacca, and Professor A. Sabatini for their generous support of the program SUPERQUAD.

(40) Braibanti, A.; Dallavalle, F.; Leporati, E.; Mori, G. *J. Chem. Soc., Dalton Trans.* **1973**, 2539.
(41) Braibanti, A.; Dallavalle, F.; Leporati, E.; Mori, G. *J. Chem. Soc., Dalton Trans.* **1973**, 323.
(42) Braibanti, A.; Mori, G.; Dallavalle, F.; Leporati, E. *Inorg. Chim. Acta* **1972**, *6*, 106.
(43) Braibanti, A.; Dallavalle, F.; Leporati, E. *Inorg. Chim. Acta* **1969**, *3*, 459.
(44) De Miranda Pinto, C. O.; Paniago, E. B.; Tabak, M.; Carvalho, S.; Mascarenhas, Y. P. *Inorg. Chim. Acta* **1987**, *137*, 145.
(45) El-Ezaby, M. S.; Marafie, H. M.; Abud-Soud, H. M. *Polyhedron* **1986**, *5*, 973.
(46) *SAS User's Guide: Statistics*, Version 5; SAS Institute Inc.: Cary, NC, 1985; p 576.

Contribution from the Institute for Physical and Theoretical Chemistry, University of Frankfurt, Niederurseler Hang, 6000 Frankfurt/Main, FRG, Institute for Inorganic Chemistry, University of Witten/Herdecke, Stockumer Strasse 10, 5810 Witten, FRG, and Institut de Chimie Minérale et Analytique, Université de Lausanne, CH-1005 Lausanne, Switzerland

Kinetics and Mechanism of Solvent-Exchange and Anation Reactions of Sterically Hindered Diethylenetriamine Complexes of Palladium(II) in Aqueous Solution

J. Berger,[1a] M. Kotowski,[1a] R. van Eldik,*[1b] U. Frey,[1c] L. Helm,[1c] and A. E. Merbach*[1c]

Received February 16, 1989

The kinetics of water exchange on and anation reactions of $[Pd(R_5dien)H_2O]^{2+}$ (R_5dien = *N,N,N',N'',N''*-pentamethyl- and *N,N,N',N'',N''*-pentaethyldiethylenetriamine) by thiourea and methyl-substituted thiourea were studied as a function of temperature and pressure. The kinetic parameters (k, ΔH^*, ΔS^*, ΔV^*) for water exchange are as follows for R = Me and Et, respectively: 187 ± 27, 2.9 ± 0.1 s^{-1}; 62 ± 3, 63 ± 1 kJ mol^{-1}; +8 ± 7, −25 ± 2 J K^{-1} mol^{-1}; −7.2 ± 0.6, −7.7 ± 1.3 cm^3 mol^{-1}. The volumes of activation for the anation reactions of the pentamethyl and pentaethyl complexes are as follows (cm^3 mol^{-1}) for anation by thiourea, dimethylthiourea, and tetramethylthiourea, respectively: −9.3 ± 0.4, −8.3 ± 0.3; −9.1 ± 0.6, −10.2 ± 0.6; −13.4 ± 0.7, −12.7 ± 0.6. The negative volumes of activation are consistent with an associative mode of activation for both processes. Steric hindrance on either the dien ligand or the entering nucleophile does not affect the associative nature of the substitution process.

Introduction

Numerous studies from our laboratories and others have demonstrated the importance of including pressure as a kinetic parameter in the elucidation of inorganic reaction mechanisms.[2-4] These studies have especially led to a better understanding and a systematic classification of solvent-exchange and ligand-substitution reactions of octahedral complexes of transition-metal elements. It was for instance possible to reveal a mechanistic changeover for solvent-exchange and complex-formation reactions along the series of divalent first-row transition-metal complexes.[3] Furthermore, solvent-exchange reactions are of fundamental importance to ligand-substitution reactions that involve the replacement of a solvent molecule. They act as model systems for ligand-substitution reactions in which both the entering and leaving ligands are neutral molecules.

Some of us[1a,b] have a longstanding interest in the substitution behavior of sterically hindered diethylenetriamine complexes of palladium(II). Aspects that were investigated include spontaneous solvolysis reactions,[5,6] anation by anionic nucleophiles,[7] reactions

(1) (a) University of Frankfurt. (b) University of Witten/Herdecke. (c) Université de Lausanne.
(2) van Eldik, R., Ed. *Inorganic High Pressure Chemistry: Kinetics and Mechanisms*; Elsevier: Amsterdam, 1986; Chapters 2-4, and references cited therein.
(3) Merbach, A. E. *Pure Appl. Chem.* **1987**, *59*, 161.
(4) van Eldik, R.; Asano, T.; le Noble, W. J. *Chem. Rev.* **1989**, *89*, 549.

0020-1669/89/1328-3759$01.50/0